Kinematic Simulation for stably stratified and rotating turbulence

F. Nicolleau * and G. Yu* and J. C. Vassilicos***

* *Department of Mechanical Engineering, University of Sheffield Mapping Street, Sheffield, S1 3JD, UK*

*** *Department of Aeronautics, Imperial College of Science, Technology and Medicine, Prince Consort Road, South Kensington, London SW7 2BY, UK*

Abstract

The properties of one-particle and particle-pair diffusion in rotating and stratified turbulence are studied by applying the Rapid Distortion Theory to a Kinematic Simulation of the Boussinesq equation with a Coriolis term.

Scalings for one- and two-particle horizontal and vertical diffusions in purely rotating turbulence are proposed for small Rossby numbers.

Particular attention is given to the locality-in-scale hypothesis for two-particle diffusion in purely rotating turbulence both in the horizontal and the vertical directions. It is observed that both rotation and stratification decrease the pair diffusivity and improve the validity of the locality-in-scale hypothesis. In the case of stratification the range of scales over which the locality-in-scale hypothesis is observed is increased.

It is found that rotation decreases the diffusion in the horizontal direction as well as, though to a much lesser extent, in the vertical direction.

Key words: Kinematic Simulation, Rapid Distortion, Rotation, Stratification, Particle Diffusion

1 Introduction

Rapidly rotating turbulence with or without stratification is to be found in many geophysical or industrial flows. Ideally, one would like to solve exactly the governing equations resolving all the turbulence scales without having

* Email address: F.Nicolleau@Sheffield.ac.uk

recourse to simplifying assumptions. But solving directly the governing equations for such turbulent flows at Reynolds numbers of interest for practical applications will remain unfeasible for quite a long time. (See for example Kimura & Herring, 1996; Godeferd & Staquet, 2003; Kimura & Herring, 1999; Cambon *et al.*, 2004, for DNS in stratified and rotating turbulence.) So it is worth considering alternative approaches while bearing in mind that all current techniques for simulating these flows have limitations.

For example, even in the case of an idealised homogeneous turbulence, Direct Numerical Simulations have severe limitations, as far as rotating turbulence with or without stratification is concerned: (i) if the turbulence is forced, then the artificial DNS forcing should be of such a nature as not to interfere with the natural anisotropy of the turbulence as dictated by the rotation and stratification, (ii) if the turbulence is decaying, then the periodic boundary conditions can be expected to interfere with the decay unless DNSs with very large grids were possible, but they are not for a foreseeable future. (See for example Yokokawa *et al.* (2002) who achieved high-resolution direct numerical simulations of incompressible turbulence with numbers of grid points up to 4096^3 which is the limit of what is currently possible, that is $R_\lambda \simeq 1227$ for a turbulence without stratification or rotation.)

As a result of these limitations, there is scope for new simulation approaches. Kinematic Simulation (KS) is one such approach and we propose to use it to investigate the effect of strong stratification and rotation on turbulent (1-particle and 2-particle) diffusion. More precisely, We want to investigate the scaling laws for the diffusion and the locality-in-scale assumption for the separation of particle pairs. (By locality-in-scale assumption we mean the assumption that the separation process is dominated by eddies with size of order the pair separation). Kinematic Simulation possesses information at all scales of turbulence (i. e. eddies) which makes it a suitable candidate for that sort of study. As we mentioned previously, all techniques have their limitations: our KS is only valid for strong stratification and rotation and requires strong assumptions about input energy spectra. However, little is known about energy spectra in rotating turbulence. Let us mention some laboratory works on stratified turbulence, e. g. the most recent work of Praud *et al.* (2005) who mention an asymptotic k^{-2} horizontal power spectrum and a k^{-3} vertical power spectrum. There are also some results from atmospheric turbulence, see Lindborg (2002), for instance, who mentions clear $k^{-5/3}$ horizontal power spectra from (Nastrom & Gage, 1985) and k^{-3} vertical power spectra from (Cot, 2001).

It is important to point out that these typical power laws (k^p) reflect a highly - but simplified - anisotropic structure. It is the simplest kind of anisotropy consistent with the governing equations. The ultimate spectral information would be given by a three-dimensional energy spectrum or $e(k_\parallel; k_\perp)$, where $k_\parallel$ and $k_\perp$ are respectively the projection of $\mathbf{k}$ on the vertical and horizontal axes. The

classical energy spectrum $E(k)$ (the only one relevant in isotropic turbulence) is obtained by averaging $e(k_\parallel; k_\perp)$ over spheres. Horizontal and vertical spectra are obtained by averaging over planes or cylinders in the three-dimensional Fourier space, therefore mixing different angular information. This underlying anisotropic aspect is often ignored. It is worth mentioning here some attempts at filling the gap between pure isotropic 3D and pure 2D in rotating turbulence: an asymptotic wave-turbulence approach by Bellet *et al.* (2006) and the DNS by Liechtenstein *et al.* (2006).

It is also worth remembering that atmospheric turbulence is non-decaying, whereas laboratory experiments on rotating turbulence with or without stratification are. Furthermore, to our knowledge, there is no clear experimental evidence as to the effect on the spectrum power law of adding rotation to a stratified turbulence.

When using KS, we have to make assumptions on the input energy spectrum. It would be possible to render the KS consistent with a prescribed fully anisotropic distribution $e(k_\parallel; k_\perp)$. Although, we expect the spectra to affect our results for pair diffusion, there is no results either from DNS or laboratory to compare our results with. So, we leave fully anisotropic distribution for future studies and as a first step in this paper effectively we assume a $k^{-5/3}$ dependence with no dependence on Reynolds, Froude and Rossby numbers. Our simulations can be run again with different assumed energy spectra and therefore the methodology presented is of value as the KS can be run again when more information is known about energy spectra.

So, we present these results with the caveat that some of them may be different in reality if the spectra are different functions of wavenumber, Reynolds, Froude and Rossby number than the ones we assume in our input. For the 2-particle results, we know where most of the uncertainty comes from in the assumptions, the energy spectrum, and the calculations can be easily repeated with different energy spectra. Still, our 2-particle results are interesting because they reveal interesting new effects, which, at the very least, can serve as new questions and concepts for the study of pair-diffusion in rapidly rotating turbulence with or without stratification.

Whenever possible we compared our results with DNS. For these cases, KS predictions of one-particle and two-particle dispersion match the DNS predictions for stratified turbulence, this was reported in (Godeferd *et al.*, 1997; Nicolleau & Vassilicos, 2000). KS also matches DNS predictions of one-particle dispersion in pure rotation and rotating stratified turbulence as reported in (Cambon *et al.*, 2004). The KS results for two-particle dispersion in purely rotating turbulence presented in this latter paper are also in agreement with the DNS predictions of (Kimura & Herring, 1999).

Strongly stratified turbulence can be found inside the oceans, however rapidly rotating turbulence (small Rossby numbers) can only be found at large scales where rotation is spatially varying. Another example of such turbulence would be flows inside engines but these are much more complex than the homogeneous flows considered in this paper. We assume a rotation rate that is space independent in line with existing DNS simulations (Kimura & Herring, 1999; Cambon *et al.*, 2004); in that sense our work may seem of no direct applicability in the physical world where it is hard to find such flows, but this is a start, and we might expect space-dependencies to give small corrections to the main ones generated by the constant rotation. We expect this to be all the more true as our work shows the preponderance of the linear terms as far as Lagrangian tracking is concerned.

KS is very good at picking up the role of linear terms and our results show that these terms can explain a lot concerning 1 and 2 particle diffusion. Our approach is to understand fully their role before moving on to the exact role of the energy spectrum's power law.

In order to derive Lagrangian trajectories and statistics, if one starts from Eulerian based methods there is only one approach: compute with a full resolution all large scales and model the smallest ones. Then, either the Reynolds number has to be small or the effect of the smallest scales - the one modelled in the Eulerian computation - have to be discarded or modelled. Kinematic Simulation (KS) as a Lagrangian model implements a different modelling strategy. In order to derive the Lagrangian trajectories one has to integrate the Eulerian velocity field:

$$\frac{d\mathbf{x}}{dt} = \mathbf{u}(\mathbf{x}, t) \tag{1}$$

knowing the initial conditions for the fluid element (alias particle in this paper) $\mathbf{x}_0$. After its release the particle will experience the action of all of turbulence's scales, and KS must therefore retain information about all scales not only large ones. Hence in KS the velocity field $\mathbf{u}(\mathbf{x}, t)$ is modelled with the same accuracy from the largest down to the smallest scale.

Kinematic Simulations (KS) were first developed for homogeneous isotropic turbulence where incompressibility and an energy power law spectrum were prescribed (e.g. Fung *et al.*, 1992; Elliott & Majda, 1996; Fung & Vassilicos, 1998, and references therein). It appears from (Malik & Vassilicos, 1996; Flohr & Vassilicos, 2000; Nicolleau & ElMaihy, 2004) that for many Lagrangian properties no particular time-dependence needs to be introduced and a 'frozen' 3-D Eulerian velocity field can generate many Lagrangian properties of the turbulence. The three-dimensionality of streamlines ensures all the necessary time-decorrelations to obtain ballistic régime, random walk régime and Richardson régime for particle pairs initially separated by η the Kolmogorov length scale (Nicolleau & Yu, 2004). Thomson & Devenish (2005) argue for a $t^{9/2}$-regime

rather than the t^3 Richardson regime in KS. However, Osborne *et al.* (2006) have confirmed Nicolleau & Yu (2004)'s observation that the Richardson law can be captured by KS in the scaling of the pair diffusivity even when it cannot be captured in the scaling of the mean square separation itself because of contaminations by the initial separation. The results of Thomson & Devenish (2005) are concerned with the mean square separation rather than with the pair diffusivity and use an adaptive time step which, as Osborne et al (2006) have shown, can be responsible for $t^{9/2}$ scalings.

For stably stratified flows an analysis of the Lagrangian velocity time-correlation (Kaneda & Ishida, 2000; Nicolleau & Vassilicos, 2000; Cambon *et al.*, 2004) shows that its time-dependence is far more complex than for homogeneous isotropic turbulence and is crucial for the prediction of particle diffusion along the axis of stratification. (Nicolleau & Vassilicos, 2000) was one of the first attempts to extend KS to stably stratified flows. These authors implemented the time evolution predicted by Rapid Distortion Theory (RDT)'s solution of the Boussinesq equation with the KS 3-D velocity field formalism. In the present paper we extend their work to flows subjected to a rotation. Comparisons of results from KS-with-RDT [1] and results from RDT and DNS can be found in (Cambon *et al.*, 2004), additional DNS results can also be found in (Kimura & Herring, 1999).

We investigate one and two-particle diffusion along the vertical axis and in the plane orthogonal to the vertical axis. The rotation $\mathbf{\Omega}$, gravity and mean density gradient are all in the direction of the vertical axis referred to as the third axis throughout this paper: $\mathbf{\Omega} = (0, 0, \Omega)$, $\mathbf{g} = (0, 0, -g)$. The stratification is stable and the turbulence non-decaying.

In § 2 we introduce the KS model and discuss its extension to rotation. In § 3 we introduce the locality-in-scale assumption as it is to be discussed in this paper and generalise Nicolleau & Yu (2004)'s study of pair diffusion to the horizontal pair diffusion in stratified turbulence. The pure rotation's effect on turbulent diffusion is studied in § 4 for one-particle statistics and in § 5 for the particle-pair statistics. Section 6 summarises this paper's main conclusions.

2 Equations

Our KS is based on the Boussinesq assumption. We consider a stably stratified fluid at static equilibrium, with pressure $p(x_3)$ and density $\rho(x_3)$ varying only in the direction of stratification that is along the vertical axis x_3 (see

[1] For sake of simplification we keep the expression KS even when it is coupled with RDT for applications to stratified or rotating flows.

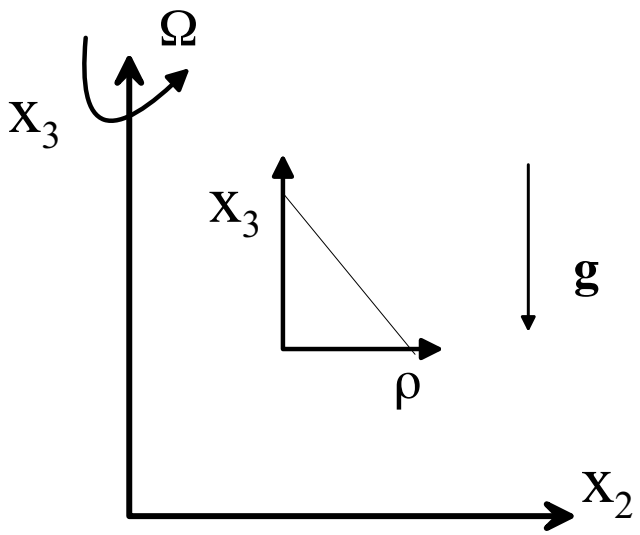

Fig. 1. Stratification and rotation direction.

figure 1). Hence $dp/dx_3 = -\rho g$ where $\mathbf{g} = (0, 0, -g)$ is the gravitational acceleration and we set $\mathbf{x} = (x_1, x_2, x_3)$ in cartesian coordinates. Under Boussinesq approximation the perturbation density ρ' is assumed much smaller that the density ρ so that

$$\frac{D}{Dt}\Theta = -u_3 \frac{1}{\rho}\frac{d\rho}{dx_3} \tag{2}$$

where $\Theta = \frac{\rho'}{\rho}$. The rotation intervenes as a corriolis term $2\mathbf{\Omega} \times \mathbf{u}$ superimposed on the stratified flow dynamics:

$$\frac{D\mathbf{u}}{Dt} = -\frac{1}{\rho}\nabla p' + \Theta\mathbf{g} - 2\mathbf{\Omega} \times \mathbf{u}, \tag{3}$$

with $\mathbf{\Omega}$ the rotation vector. In this paper the study is limited to a rotation in the direction of stratification that is $\mathbf{\Omega} = (0, 0, \Omega)$. As in (Nicolleau & Vassilicos, 2000) for sake of simplicity we omit terms describing molecular diffusion and viscosity. Though there is no theoretical difficulty to incorporate these terms, in practice they make computations rather cumbersome. The perturbation velocity $\mathbf{u}(\mathbf{x}, t)$ is also assumed incompressible:

$$\nabla.\mathbf{u} = 0 \tag{4}$$

Setting $\mathbf{a} = (a_1, a_2, a_3) = -\frac{1}{\rho}\nabla\, p'$, the Lagrangian counterparts of the Boussinesq Eulerian equations (2), (3) and (4) are

$$\ddot{x}_1(t) = a_1(t) + 2\Omega u_2(\mathbf{x}, t) \tag{5}$$
$$\ddot{x}_2(t) = a_2(t) - 2\Omega u_1(\mathbf{x}, t) \tag{6}$$
$$\ddot{x}_3(t) = a_3(t) - \Theta(t)g \tag{7}$$
$$\dot{\Theta}(t) = \frac{u_3(t)}{H} \tag{8}$$

where $a_i(t)$, $\Theta(t)$ and $u_3(t)$ are the values of a_i $(i = 1, 2, 3)$, Θ and u_3 at the points visited by fluid element trajectories at time t and $H = \rho/|d\rho/dx_3|$. Note that only the equations for horizontal motion (5) and (6) are affected by Ω. The Lagrangian Boussinesq equation for the vertical diffusion is obtained from (7) and (8) and does not explicitly depend on Ω:

$$\ddot{x}_3 = a_3 - N^2(x_3 - x_3(t_0)) - g\Theta(t_0) \tag{9}$$

where $N^2 = \frac{g}{H} = \frac{g|\frac{d\rho}{dx_3}|}{\rho}$ and t_0 is the time of release.

2.1 Pressure

The incompressibility requirement (4) imposes a coupling between vertical and horizontal displacements and a dependence of the vertical pressure acceleration a_3 on both. Indeed, the incompressibility requirement (4) applied to (3) implies that

$$-\nabla^2 p' = \rho g \frac{\partial \Theta}{\partial x_3} + \rho \frac{\partial u_j}{\partial x_i}\frac{\partial u_i}{\partial x_j} + 2\Omega\left(\frac{\partial u_1}{\partial x_2} - \frac{\partial u_2}{\partial x_1}\right) \tag{10}$$

with a summation over i, j. This Poisson equation is readily solved by Fourier transformation leading to the Lagrangian vertical pressure acceleration:

$$\begin{aligned} a_3(t) = -\tfrac{1}{\rho}\tfrac{\partial}{\partial x_3}p' &= g\int d\mathbf{k}\, e^{i\mathbf{k}.\mathbf{x}}\tfrac{{k_3}^2}{k^2}\tilde{\Theta}(\mathbf{k},t) \\ &+ i\int d\mathbf{k}\, e^{i\mathbf{k}.\mathbf{x}}\tfrac{k_3}{k^2}\int d\mathbf{k}' k_i'(k_j - k_j')\tilde{u}_j(\mathbf{k}',t)\tilde{u}_i(\mathbf{k}-\mathbf{k}',t) \\ &+ 2\Omega\int d\mathbf{k}\, e^{i\mathbf{k}.\mathbf{x}}\tfrac{k_3}{k^2}(k_2\tilde{u}_1(\mathbf{k},t) - k_1\tilde{u}_2(\mathbf{k},t)) \end{aligned} \tag{11}$$

where $\tilde{\Theta}(\mathbf{k},t)$ and $\tilde{u}_i(\mathbf{k},t)$ are the Fourier transforms of $\Theta(\mathbf{x},t)$ and $u_i(\mathbf{x},t)$ respectively with wavenumber $\mathbf{k} = (k_1, k_2, k_3)$ and $k^2 = \mathbf{k}.\mathbf{k}$. The dependence of a_3 on *both* the vertical and horizontal components of $\mathbf{x}(t)$ is manifest in (11).

2.2 Linearised Boussinesq equations with rotation

Consider an initial velocity field $\mathbf{u}(\mathbf{x}, 0)$ with spatial fluctuations over a wide range of length-scales, the smallest of these length-scales being η. In the limit where the microscale Froude number and the microscale Rossby number are much smaller than 1, i.e. $Fr_\eta \equiv \frac{u(\eta)}{N\eta} \ll 1$ and $Ro_\eta \equiv \frac{u(\eta)}{\Omega\eta} \ll 1$, (where $u(\eta)$ is the characteristic initial velocity fluctuation at scale η), the Eulerian Boussinesq equations (2) and (3) may be approximated by their linear counterparts

$$\frac{\partial}{\partial t}\Theta = -u_3\frac{1}{\rho}\frac{d\rho}{dx_3} \tag{12}$$

$$\frac{\partial}{\partial t}\mathbf{u} = -\frac{1}{\rho}\nabla p' + \Theta\mathbf{g} - 2\mathbf{\Omega}\times\mathbf{u} \tag{13}$$

We use the Fourier transform $\tilde{\mathbf{u}}(\mathbf{k},t)$ of $\mathbf{u}(\mathbf{x},t)$ to solve equations (12) and (13) so that the incompressibility constraint (4) is transformed into $\mathbf{k}.\tilde{\mathbf{u}}(\mathbf{k},t)=0$ whilst the pressure field gradient is transformed into a vector parallel to $\mathbf{k}$ in Fourier space. Setting $\mathbf{e_3}$ as the unit vector in the direction of stratification and $\mathbf{e_1}$, $\mathbf{e_2}$ two unit vectors normal to each other and to $\mathbf{e_3}$ (so that $\mathbf{x} = x_1\mathbf{e_1} + x_2\mathbf{e_2} + x_3\mathbf{e_3}$ and $\mathbf{g} = -g\mathbf{e_3}$), the Craya-Herring frame (see figure 2) is given by the unit vectors $\hat{\mathbf{k}} = \frac{\mathbf{k}}{k}$, $\mathbf{c_1} = \frac{\mathbf{e_3}\times\mathbf{k}}{|\mathbf{e_3}\times\mathbf{k}|}$ and $\mathbf{c_2} = \frac{\mathbf{k}\times\mathbf{c_1}}{|\mathbf{k}\times\mathbf{c_1}|}$. In the Craya-

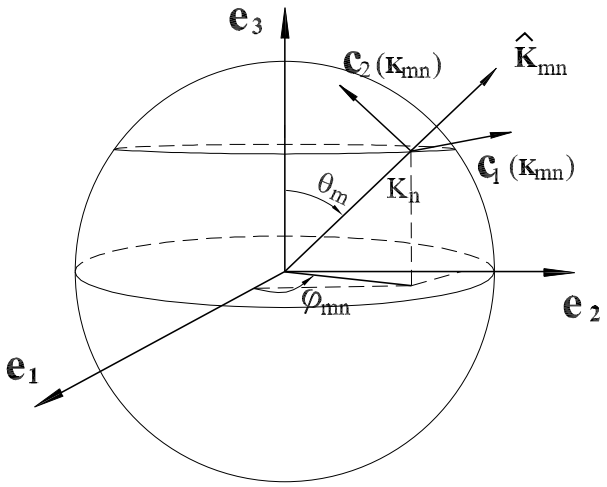

Fig. 2. Craya-Hering frame and Fourier space discretisation.

Herring frame the Fourier transformed velocity field $\tilde{\mathbf{u}}(\mathbf{k},t)$ lies in the plane defined by $\mathbf{c_1}$ and $\mathbf{c_2}$, i.e.

$$\tilde{\mathbf{u}}(\mathbf{k},t) = \tilde{v}_1(\mathbf{k},t)\mathbf{c_1} + \tilde{v}_2(\mathbf{k},t)\mathbf{c_2}, \tag{14}$$

and is therefore decoupled from the pressure fluctuations which are along $\mathbf{k}$. It is worth mentioning here the linkage of this Craya-Herring frame to a precise wave-vortex decomposition (see, e.g. Cambon *et al.* (2004); Liechtenstein *et al.* (2006)). $\mathbf{c_1}$ corresponds to a 'vertical vortex' or toroidal mode, whereas $\mathbf{c_2}$ corresponds to a wave or poloidal mode. Incompressible solutions of equations (12) and (13) in Fourier space and in the Craya-Herring frame are (Godeferd & Cambon, 1994):

$$\begin{aligned}\tilde{v}_1(\mathbf{k},t) = {} & \tfrac{{\sigma_s}^2}{\sigma^2}\tilde{v}_1(\mathbf{k},0) - \tfrac{\sigma_r\, g\sin\theta}{\sigma^2}\tilde{\Theta}(\mathbf{k},0) \\ & + \left(\tfrac{{\sigma_r}^2}{\sigma^2}\tilde{v}_1(\mathbf{k},0) + \tfrac{\sigma_r\, g\sin\theta}{\sigma^2}\tilde{\Theta}(\mathbf{k},0)\right)\cos\sigma t \\ & + \tfrac{\sigma_r}{\sigma}\tilde{v}_2(\mathbf{k},0)\sin\sigma t\end{aligned} \tag{15}$$

$$\tilde{v}_2(\mathbf{k},t) = \tilde{v}_2(\mathbf{k},0)\cos\sigma t - \left(\frac{\sigma_r}{\sigma}\tilde{v}_1(\mathbf{k},0) + \frac{g\sin\theta}{\sigma}\tilde{\Theta}(\mathbf{k},0)\right)\sin\sigma t \tag{16}$$

$$\begin{aligned}\tilde{\Theta}(\mathbf{k},t) = & -\tfrac{N}{g}\tfrac{\sigma_r\sigma_s}{\sigma^2}\tilde{v}_1(\mathbf{k},0) + \tfrac{{\sigma_r}^2}{\sigma^2}\tilde{\Theta}(\mathbf{k},0) \\ & + \tfrac{N}{g}\tfrac{\sigma_s}{\sigma^2}\left(\sigma_r\tilde{v}_1(\mathbf{k},0) + g\sin\theta\ \tilde{\Theta}(\mathbf{k},0)\right)\cos\sigma t \\ & + \tfrac{N}{g}\tfrac{\sigma_s}{\sigma}\tilde{v}_2(\mathbf{k},0)\sin\sigma t\end{aligned} \tag{17}$$

where $\theta = \theta(\mathbf{k})$ is the angle between $\mathbf{k}$ and $\mathbf{e_3}$, $\sigma_r = 2\Omega\cos\theta$, $\sigma_s = N\sin\theta$, $\sigma = \sqrt{{\sigma_r}^2 + {\sigma_s}^2}$, and the initial conditions are $\tilde{v}_1(\mathbf{k},0)$, $\tilde{v}_2(\mathbf{k},0)$ and $\tilde{\Theta}(\mathbf{k},0)$.

In this paper the study is limited to the case $\tilde{\Theta}(\mathbf{k},0) = 0$ (zero initial potential energy), in which case the equations (15), (16), (17) become

$$\tilde{v}_1(\mathbf{k},t) = \frac{{\sigma_s}^2}{\sigma^2}\tilde{v}_1(\mathbf{k},0) + \frac{{\sigma_r}^2}{\sigma^2}\tilde{v}_1(\mathbf{k},0)\cos\sigma t + \frac{\sigma_r}{\sigma}\tilde{v}_2(\mathbf{k},0)\sin\sigma t \tag{18}$$

$$\tilde{v}_2(\mathbf{k},t) = \tilde{v}_2(\mathbf{k},0)\cos\sigma t - \frac{\sigma_r}{\sigma}\tilde{v}_1(\mathbf{k},0)\sin\sigma t \tag{19}$$

$$\begin{aligned}\tilde{\Theta}(\mathbf{k},t) = & -\frac{N}{g}\frac{\sigma_r\sigma_s}{\sigma^2}\tilde{v}_1(\mathbf{k},0) + \frac{N}{g}\frac{\sigma_s\sigma_r}{\sigma^2}\tilde{v}_1(\mathbf{k},0)\cos\sigma t \\ & + \frac{N}{g}\frac{\sigma_s}{\sigma}\tilde{v}_2(\mathbf{k},0)\sin\sigma t\end{aligned} \tag{20}$$

2.3 KS velocity field

We generalise Nicolleau & Vassilicos (2000)'s KS velocity field for stratified turbulence. Here, a homogeneous isotropic turbulent field is subjected to rotation with or without stratification. The KS model of turbulent diffusion in rotating or/and stratified non-decaying turbulence consists in solving

$$\frac{d\mathbf{x}}{dt} = \mathbf{u}(\mathbf{x}(t),t) \tag{21}$$

to obtain an ensemble of Lagrangian trajectories $\mathbf{x}(t)$ from the velocity field

$$\begin{aligned}\mathbf{u}(\mathbf{x},t) = 2\pi\Re\Big\{\textstyle\sum_{n=1}^{N_k}\sum_{m=1}^{M_\theta}\ {k_n}^2\sin\theta_m\Delta k_n\Delta\theta_m e^{i\mathbf{k_{mn}}.\mathbf{x}} \\ [\tilde{v}_1(\mathbf{k_{mn}},t)\mathbf{c_1}(\mathbf{k_{mn}}) + \tilde{v}_2(\mathbf{k_{mn}},t)\mathbf{c_2}(\mathbf{k_{mn}})]\Big\}\end{aligned} \tag{22}$$

where $\mathbf{k}_{mn}$ has magnitude k_n and direction given by θ_m and ϕ_{mn} (see figure 2) where ϕ_{mn} is chosen randomly, $\Delta k_n = k_{n+1} - k_n$, $\Delta\theta_m = \theta_{m+1} - \theta_m$ and $\Re$ stands for the real part, $\tilde{v}_1(\mathbf{k_{mn}},t)$ obeys equation (18) and $\tilde{v}_2(\mathbf{k_{mn}},t)$ equation (19). (We refer the reader to Nicolleau & Vassilicos (2000) for details of the KS discretisation.) $\tilde{v}_1(\mathbf{k_{mn}},0)$, $\tilde{v}_2(\mathbf{k_{mn}},0)$ are specified initial conditions randomly

chosen in accordance with an energy spectrum $E(k)$ that has a $-5/3$ large-wavenumber scaling, that is:

$$E(k)\begin{cases} \sim k^{-\frac{5}{3}} \quad \text{for} \quad k_1 \leq k \leq k_{N_k} \equiv \frac{2\pi}{\eta} \\ = 0 \qquad\qquad\quad \text{otherwise} \end{cases} \tag{23}$$

The spectrum is characterised by the rms value of the velocity fluctuation

$$u'^2 = \frac{2}{3}\int E(k)dk, \tag{24}$$

the integral length-scale

$$L = \frac{3\pi}{4}\frac{\int k^{-1}E(k)dk}{\int E(k)dk}, \tag{25}$$

of the initial isotropic turbulence and the Kolmogorov length scale η. We also introduce t_d the eddy turnover time associated to L and u' as follows

$$t_d = \frac{L}{u'} \tag{26}$$

and τ_η the characteristic time associated to the inner (viscosity simulating) length-scale:

$$t_\eta = \left(\frac{\eta}{L}\right)^{\frac{2}{3}} t_d \tag{27}$$

In this paper we choose the values $M_\theta = 20$ and $N_k = 50$ for the cases with stratification. For pure rotation it was found that a refined discretisation of the angles θ is needed and we choose $M_\theta = 100$ and $N_k = 30$

Velocity correlations were tested against RDT and DNS results. They have shown satisfactory agreement for cases $\frac{2\Omega}{N} = 0$, 0.1 and ∞ (see Cambon *et al.*, 2004, for details).

For sake of simplicity we introduce the following notations

$$\begin{cases} \tau & = t - t_0 \\ \zeta_i(\tau) & = x_i(t) - x_i(t_0) \\ \Delta_i(\tau) & = x_i^1(t) - x_i^2(t) \\ \Delta^2 & = \Delta_1^2 + \Delta_2^2 + \Delta_3^2 \\ \Delta_0 & = |\mathbf{x}^1(0) - \mathbf{x}^2(0)| \\ \Delta_i^r(\tau) & = (x_i^1(t) - x_i^1(t_0)) - (x_i^2(t) - x_i^2(t_0)) \\ \delta_i(\tau) & = \sqrt{< \Delta_i(t)^2 >} \\ \delta_i^r(\tau) & = \sqrt{< \Delta_i^r(t)^2 >} \end{cases} \tag{28}$$

where t_0 is the time of release of the particle, x_i is the ith component of the particle's position vector $\mathbf{x}$, $\mathbf{x^1}$ refers to the first particle of the particle-pair and $\mathbf{x^2}$ to the second particle of the pair. Subscripts h and v when they are substituted to i indicate respectively any horizontal direction properties and the vertical properties. For example Δ_h represents the separation in any direction on the horizontal plane, i.e., $< \Delta_h^2 >=< \Delta_1^2 >=< \Delta_2^2 >$. The strength of the stratification is characterised by the Froude number Fr:

$$Fr = \frac{u'}{LN} \tag{29}$$

and the strength of the rotation by the Rossby number Ro:

$$Ro = \frac{u'}{2L\Omega} \tag{30}$$

In order to make the RDT valid, the Froude number or the Rossby number should be smaller than 1 at all scales, and we matched that criteria for all the cases presented in this paper. In practice, we expect our results to be also valid for the larger scales of real flows, where Fr and Ro may be larger than 1 at the smallest scales, as we have observed that breaking the criteria $Fr < 1$, $Ro < 1$ at small scales does not affect the results at large scales.

3 Additional results for particle-pair diffusion in purely stratified turbulence

One and two-particle diffusion in stratified turbulence using KS was first studied in (Nicolleau & Vassilicos, 2000) where it was shown that:

Case	N	L	u'	$\frac{1}{\eta}$	$\frac{\Delta_0}{\eta}$	Fr
A	1250	0.5	0.35	25	1	0.00056
B	2500	0.25	0.35	25	1	0.00056
C	2500	0.5	0.175	25	1	0.00014
D	2500	0.5	0.35	50	1	0.00028
E	2500	0.5	0.35	25	1	0.00028
F	2500	0.5	0.35	25	10	0.00028
G	2500	0.5	0.35	25	0.1	0.00028
H	2500	0.5	0.35	25	0.01	0.00028
I	1250	0.5	0.35	25	0.1	0.00056
J	500	0.5	0.35	25	0.1	0.0014

Table 1
Different cases studied for particle-pair diffusion in purely stratified turbulence

i) the one-particle diffusion in the horizontal plane is not altered by stratification. It first follows a ballistic régime characterised by a τ^2-law up to a time of the order of $\frac{L}{u'}$ and then it follows a random walk diffusion characterised by a τ-law.
ii) The one-particle vertical diffusion is bounded. It first follows a ballistic régime up to a characteristic time of the order of $\frac{1}{N}$ and then levels off on a plateau diffusion of the order of $\frac{u'^2}{N^2}$. This plateau can be predicted using energy arguments: the conservation of energy imposes that the potential energy i. e. $N^2 < \zeta_v^2 >$ is bounded.
iii) The pair diffusion in the horizontal plane follows the isotropic patterns, whereas in the vertical direction it exhibits two plateaux.

In this section we concentrate on new results concerning pair horizontal diffusion in stratified turbulence. In particular, we extend Nicolleau & Yu (2004)'s study of pair diffusion to stratified turbulence and particularly focus on the locality-in-scale concept as discussed in (Nicolleau & Yu, 2004). The locality-in-scale assumption is an idea introduced by Obukhov (1941) and Batchelor (1952) according to which the pair diffusivity $\frac{d}{dt} < \Delta^2 >$ is mainly sensitive to eddies of size $\delta = \sqrt{< \Delta^2 >}$. For a turbulence spectrum $E(k) \sim k^{-\frac{5}{3}}$ it can easily be shown that this assumption leads to

$$\frac{d}{dt} < \Delta^2 >= \beta u' \eta \left(\frac{L}{\eta}\right)^{-1/3} \left(\frac{\delta}{\eta}\right)^{4/3} \tag{31}$$

and equivalently, to

$$< \Delta^2(\tau) >= G_\Delta \epsilon \tau^3 \tag{32}$$

where we neglect initial separation terms (Morel & Larchevêque, 1974; Fung & Vassilicos, 1998). For an anisotropic flow we can define a coefficient β_h based on the horizontal diffusivity as follows

$$\frac{d}{dt} < \Delta_h^2 >= \beta_h u' \eta \left(\frac{L}{\eta}\right)^{-1/3} \left(\frac{\delta_h}{\eta}\right)^{4/3} \tag{33}$$

In (Nicolleau & Yu, 2004) it was shown that the best way to estimate Richardson's locality assumption is to study Richardson's coefficient β defined by equation (31). Though the diffusivity $\frac{d}{dt} < \Delta^2 >$ and the pair rms separation δ are functions of time, time does not appear explicitly in equation (31) which simplifies greatly the study of the effect of the initial condition and enables clear conclusions on the validity of the locality-in-scale assumption. If β is constant then the locality-in-scale assumption is verified, otherwise β will measure the departure from this assumption. We also define χ_i (where $i = 1, 2, 3$ for pair-diffusion in different directions) as the range of $\frac{\delta}{\eta}$ over which the locality assumption is observed.

We assume we can extend this interpretation to stratified or rotating turbulence because:

i) here, under the Rapid Distortion assumption the initial spectrum [2] is not affected by the stratification or Rotation, KS does not change the Eulerian spectrum;
ii) in order to be valid our KS requires $Fr < 1$ and $Ro < 1$ at all scales, which means that the characteristic time scales of stratification and rotation are decoupled from the turbulence characteristic time scale;
iii) Going back to the interpretation in the Craya-Herring frame (Godeferd *et al.*, 1997), the horizontal diffusion in stratified turbulence resembles the isotropic diffusion because it is mainly driven by the 'vertical vortex' mode, which is unaffected by stratification (for $\Omega = 0$) and decoupled from wave-motion in the linear regime, i.e. it does not differ much from what would happen in an isotropic field. Nevertheless, this mode is not the whole horizontal motion in stratified turbulence, so that its efficiency to drive the diffusion is reduced with respect to the isotropic case. This supports the extension of the interpretation of (31) to (33) for the cases we are studying in this paper.

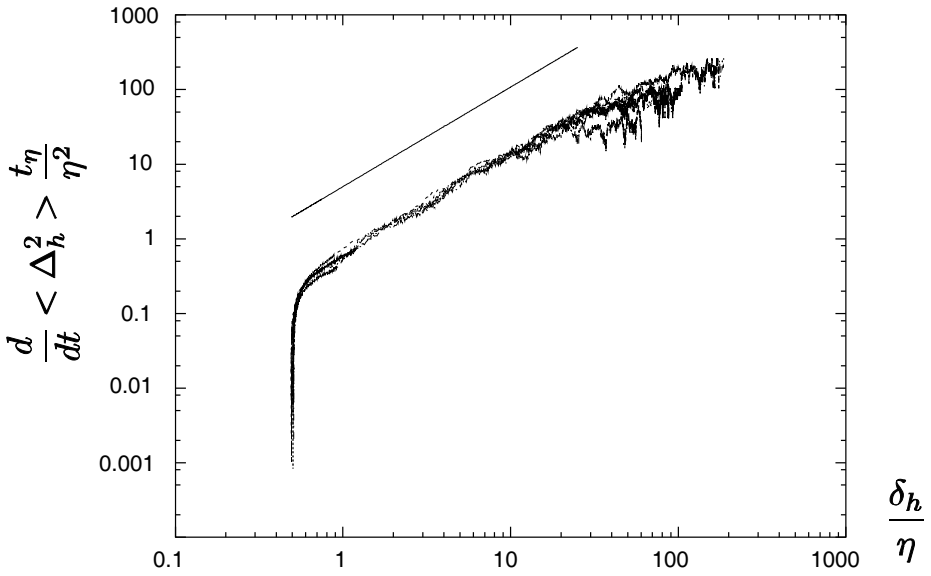

Fig. 3. Non-dimensional two-particle horizontal diffusivity $\frac{d}{dt} < \Delta_h^2 > \frac{t_\eta}{\eta^2}$ as a function of δ_h/η in purely stratified turbulence for cases A, B, C, D and E in table 1. The solid line has a 4/3-slope.

3.1 Two-particle horizontal diffusion in purely stratified turbulence

Following Nicolleau & Vassilicos (2000) particle-pairs are released at a random time large enough for the velocities to have reached their asymptotic r.m.s values as a result of rotation's and stratification's rapid distortion (see also Cambon *et al.*, 2004). Averages are then taken over 4 pairs in 250 to 30 000 realisations of turbulence depending on cases. The number of realisations needed to get converged results depends mainly on $\frac{\Delta_0}{\eta}$ and $\frac{L}{\eta}$. Figure 3 presents the results of the non-dimensional two-particle horizontal diffusivity $\frac{d}{dt} < \Delta_h^2 > t_\eta/\eta^2$ as a function of δ_h/η in purely stratified turbulence for cases A, B, C, D and E in table 1 where turbulent parameters N, L, u' and η are varied. The initial separation is kept constant for all the cases and the initial separation vector is random in 3-D space. The plot shows that there is a range in which all the curves collapse and this collapse is very close to a straight line representing Richardson's four-third diffusivity law.

The collapse in figure 3 also illustrates that Richardson's coefficient β_h as defined by (31) is independent of the turbulent parameters N, L, u' and η.

In this figure, cases A, C and E have the same $L/\eta = 12.5$ but different Froude numbers; the curves corresponding to these cases collapse in the same range

[2] The initial spectrum is the one when particles are released, in the case of stratification this is done when the kinetic energy and potential energy have reached their asymptotic value (see Nicolleau & Vassilicos (2000)).

regardless of the different Fr numbers. In case B, $L/\eta = 6.25$ and in case D, $L/\eta = 25$; case D has the longest collapse whereas case B has the shortest. So that we can conclude, at least for the cases considered in this paper i. e. provided that $Fr_\eta < 1$, that χ_h is only a function of L/η and increases with it.

To conclude accurately about the locality hypothesis, figure 4 shows β_h as a function of $\frac{\delta_h}{\eta}$ for different values of N, and an isotropic (non-stratified) case is also plotted for comparison. It shows that in the presence of stratification, β_h is reduced but much closer to a constant value suggesting that the locality-in-scale hypothesis is valid in the horizontal plane of purely stratified turbulence independently of N. Again this result can only be valid for the cases for which the KS is valid that is when $Fr_\eta < 1$. In particular such results cannot be extrapolated to $N \to 0$.

As to whether the locality-in-scale hypothesis is valid in the case of the isotropic diffusion shown in figure 4, one has to remember that β_h is on a linear scale versus a logarithmic one. We usually prefer to compare cases and rank them according to how closer they are from a constant β_h. For sake of comparison we will say here that for the isotropic case shown in figure 4 with $L/\eta = 400$ the locality-in-scale hypothesis is *only approximately valid* over a range $\chi_h = [1, 40]$. A range that is of about the same order as in the purely stratified turbulence with a much smaller inertial range $L/\eta = 12.5$. Furthermore, in purely stratified turbulence the quality of the locality-in-scale hypothesis is much improved. However, both β_h and χ_h are independent of N for all cases studied in this paper.

It should be pointed out that the above discussion is based on a fixed value of Δ_0 and it has been found in isotropic turbulent diffusion (Nicolleau & Vassilicos, 2003; Nicolleau & Yu, 2004) that the locality-in-scale hypothesis is not valid over a large portion of the inertial subrange when $\Delta_0 \leq \eta$: in this case Richardson's coefficient becomes a strong increasing function of Δ_0.

In figure 5, β_h is plotted as a function of δ_h/η for different initial separations, namely $\Delta_0/\eta = 0.01$, 0.1, 1 and 10. Two additional cases of β_h for isotropic turbulence with $\Delta_0/\eta = 1$ and 0.1 are also plotted at the top of the figure for the purpose of comparison. As in figure 4, $L/\eta = 400$ is used for the isotropic cases whilst $L/\eta = 12.5$ is used in the purely stratified turbulence cases.

For all values of $\Delta_0 \ll L$, it can also be seen in figure 5 that by contrast to the isotropic cases, there is a range where the variation of β_h with $\frac{\delta_h}{\eta}$ is small and can be neglected. In this range, β_h is δ_h-independent for all the initial separations much smaller than the integral length-scale. However, β_h remains an increasing function of Δ_0. Therefore, it can be concluded that stratification enhances Richardson's four-third diffusivity law in the horizontal direction for any initial separation $\Delta_0 \ll L$.

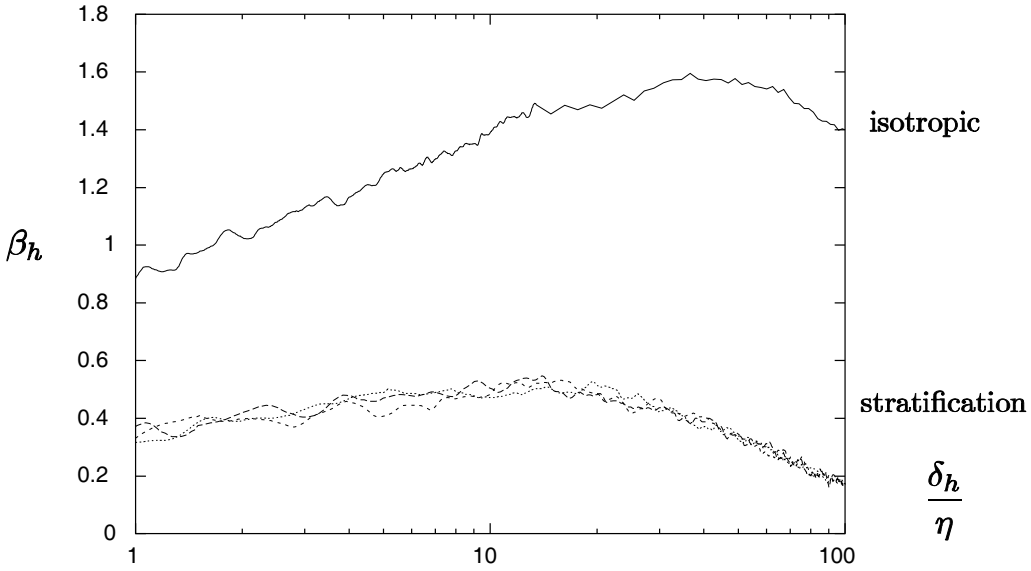

Fig. 4. Effects of N on Richardson's locality assumption at a constant $\Delta_0/\eta = 0.1$. β_h as a function of δ_h/η for case G, I, J in table 1. Other turbulent parameters are $L = 0.5$, $u' = 0.35$ and $1/\eta = 25$. An isotropic case ($N = 0$, $\Omega = 0$) with $L/\eta = 400$, $u' = 0.35$ and $\Delta_0/\eta = 0.1$ is plotted at the top for comparison.

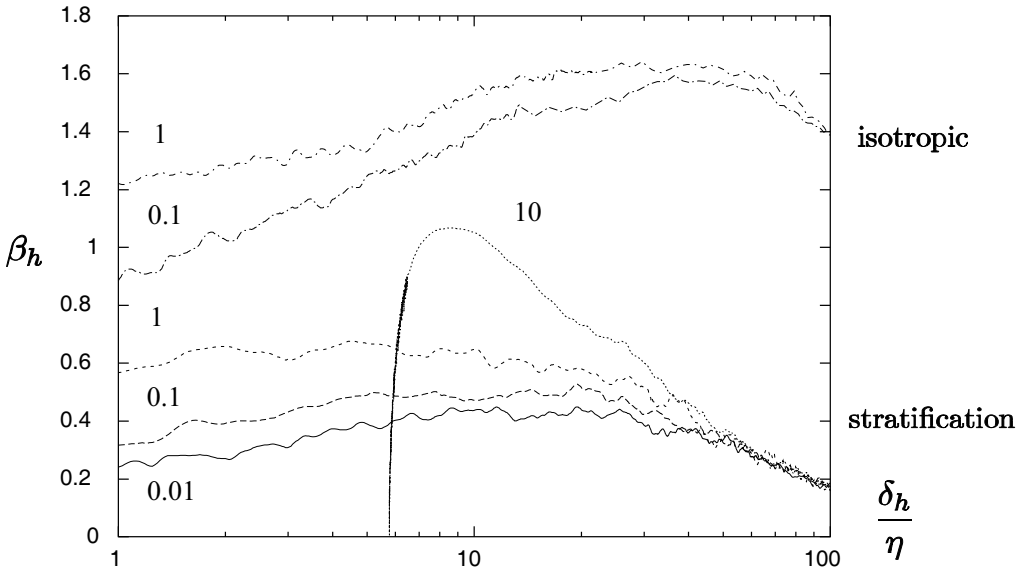

Fig. 5. β_h as a function of δ_h/η for different Δ_0/η in purely stratified turbulence at a constant Fr number. The bottom four curves are the purely stratified cases with $\Delta_0/\eta = 0.01$, 0.1, 1 and 10 from bottom to top (cases, H, G, E and F in table 1), whilst the top two curves are for the isotropic case $L/\eta = 400$, $u' = 0.35$ with respectively $\Delta_0/\eta = 1$ (top) and 0.1 (bottom).

Figure 5 also shows that the length of Richardson's four-third range χ_h has a weak dependence on the initial separation if $\Delta_0/\eta \leq 1$. However, it strongly depends on the initial separation when $\Delta_0/\eta > 1$ and decreases with it, but of course here $\frac{L}{\eta} \simeq 10$ and this strong dependence on Δ_0/η might simply be the

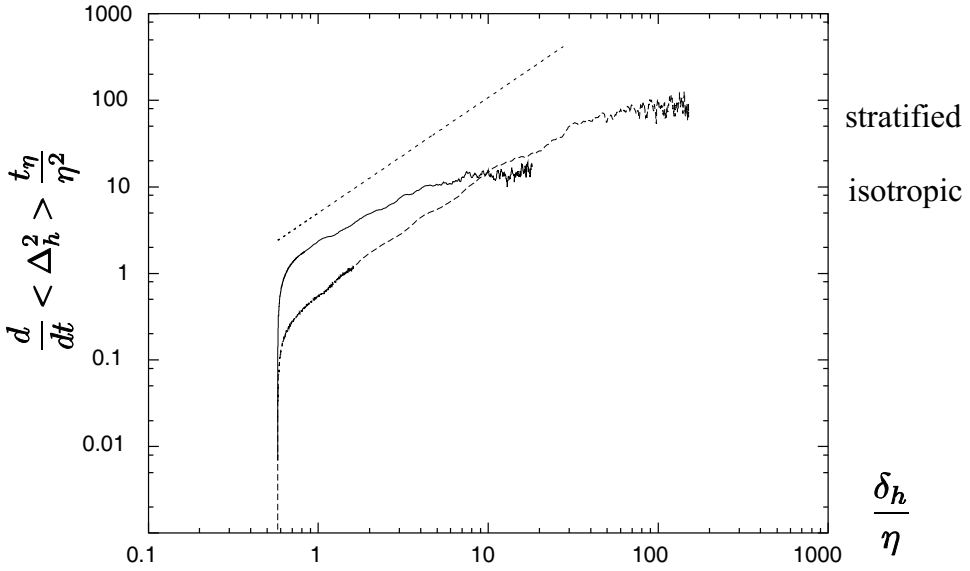

Fig. 6. Comparison of two-particle horizontal diffusivity $\frac{d}{dt} < \Delta_h^2 > \frac{t_\eta}{\eta^2}$ as a function of δ_h/η in isotropic turbulence and purely stratified turbulence with $N = 2500$. Other parameters are $L = 0.5$, $u' = 1$ and $1/\eta = 25$. $\Delta_0/\eta = 1$. Solid line is for the isotropic case, dotted line represents Richardson's four-third diffusivity law in the horizontal plane.

result of finite size effects of the inertial subrange. When $\Delta_0 \sim L$ the particles are nearly uncorrelated and are close to the random walk regime.

Further illustration of the improvement of the locality assumption with stratification is shown in figure 6. The inertial subrange ratio $L/\eta = 12.5$ is so small that for isotropic turbulent diffusion the locality assumption is hardly observed. However, in purely stratified turbulence there is a well defined four-third range that lasts up to $\delta_h/\eta \approx 30$, which demonstrates that the stratification extends the region where the locality assumption applies beyond the inertial subrange. In other words, the locality-in-scale assumption in purely stratified turbulence is not only valid inside the inertial subrange but also beyond it. This can be, at least partially, understood in terms of one-particle diffusion results such as those shown in figure 7. The particle in purely stratified turbulence reaches its random walk régime later than in isotropic turbulence. This delay allows the two particles in purely stratified turbulence to stay correlated longer, which explains the larger range where the locality assumption applies.

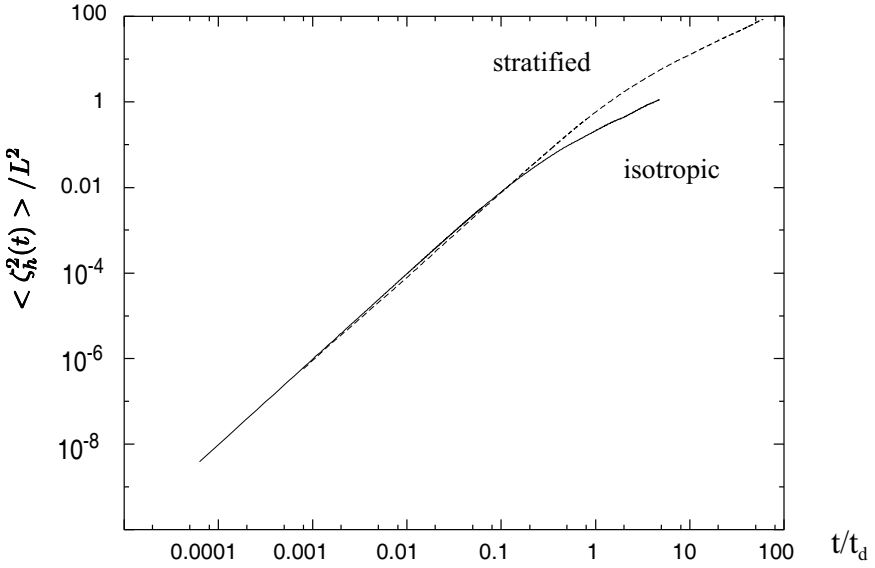

Fig. 7. Comparison of one-particle horizontal diffusion $< \zeta_h^2 > /L^2$ as a function of t/t_d in isotropic turbulence and purely stratified turbulence for the same case as in figure 6. Solid line is for the isotropic case.

4 One-particle diffusion in purely rotating turbulence

4.1 Introduction

Many cases are run to investigate the one- and two-particle diffusions in purely rotating turbulence by varying Ω, u', L, η and Δ_0. These different cases are summarized in table 2.

In figure 8 left, the non-dimensional one-particle mean square displacement $< \zeta^2(\tau) > /L^2$ in the three coordinate directions is plotted against the normalized time τ/t_d. As for purely stratified turbulence, the one-particle mean square displacement $< \zeta_h^2(\tau) >$ is identical in the two horizontal directions. By contrast to purely stratified turbulence in which the vertical diffusion is virtually suppressed by stratification after the early-time τ^2-régime, the vertical diffusion is larger than the horizontal diffusion in purely rotating turbulence. One can also see that both the horizontal and the vertical diffusions display a τ^2 ballistic régime at very small times and a random walk régime at large times.

A noticeable feature illustrated in figure 8 right is that when $\tau \gg L/u'$ the ratio of the vertical diffusion $< \zeta_v^2(\tau) >$ to the horizontal diffusion $< \zeta_h^2(\tau) >$ is 2, the analytical value predicted by Rapid Distortion Theory (RDT) and the simplified corrsin hypothesis (SCH) in (Cambon *et al.*, 2004). Following the approach developed in this latter paper, it is important to point out that, by

Case	Ω	L	u'	$\frac{1}{\eta}$	$\frac{\Delta_0}{\eta}$	Ro
A	100	0.5	2.0	250	1.0	0.02
B	100	1.0	2.0	250	1.0	0.01
C	100	0.5	2.0	125	1.0	0.02
D	100	0.5	1.0	250	1.0	0.01
E	50	0.5	2.0	250	1.0	0.04
F	100	0.5	2.0	250	0.3	0.02
G	100	0.5	2.0	250	0.02	0.02
H	100	0.5	2.0	250	10	0.02
I	400	0.5	2.0	250	1.0	0.005
J	0	0.5	2	250	0.1	∞
Case	Ω	L	u'	$\frac{1}{\eta}$	$\frac{\Delta_0}{\eta}$	Ro
K	50	1.0	2	500	1.0	0.02
L	50	1.0	2	250	1.0	0.02
M	50	0.5	1	250	1.0	0.02
N	100	0.5	2	250	1.0	0.02
O	50	0.5	2	250	0.1	0.04
P	100	0.5	2	250	0.1	0.02
Q	400	0.5	2	250	0.1	0.005
R	50	1.0	2	500	0.02	0.02
S	50	1.0	2	500	0.1	0.02
T	50	1.0	2	500	5.0	0.02

Table 2
Different cases studied for particle diffusion in purely rotating turbulence

contrast to pure stratification, for pure rotation the whole motion of the fluid is affected by inertial waves, hence both vertical and horizontal components are affected (but in a slightly different way which leads to the ratio 2).

4.2 One-particle horizontal diffusion in pure rotation

Figure 9 shows the one-particle non-dimensional horizontal diffusion $< \zeta_h^2(\tau) > \Omega^2/u'^2$ as a function of $\tau\Omega/\pi$; turbulence parameters varied are L, η, u' and Ω. With the normalization adopted in this figure, all the curves collapse together implying that $< \zeta_h^2(\tau) > \Omega^2/u'^2$ is a universal function f of $\tau\Omega/\pi$ at all times:

$$< \zeta_h^2(\tau) > \frac{\Omega^2}{u'^2} = f\left(\frac{\Omega}{\pi}\tau\right) \tag{34}$$

that is

$$\frac{< \zeta_h^2(\tau) >}{L^2} = (Ro)^2 \, f^*\left(\frac{\Omega}{\pi}\tau\right) \tag{35}$$

More precisely, this universal function is composed of two régimes:

- When $\tau \ll \pi/\Omega$ equation (35) represents a τ^2 ballistic régime and is found to be
$$< \zeta_h^2(\tau) >= u'^2\tau^2 \tag{36}$$
- Whereas when $\tau > \pi/\Omega$ equation (35) stands for a $\tau-$régime found to be
$$< \zeta_h^2(\tau) >= \frac{u'^2\tau}{\Omega} = 2\,Ro\,L^2\frac{\tau}{t_d} \tag{37}$$
The horizontal mean square displacement in the $\tau-$régime is then a function of the Rossby number, and (37) is consistent with the analytical derivation from RDT combined with SCH in (Cambon *et al.*, 2004). (Note that there was an error concerning this point in the conclusion of Cambon *et al.* (2004) who referenced a paper Nicolleau & Vassilicos 2003 which is nothing but an early version of this present paper.)

4.3 One-particle vertical diffusion in pure rotation

The one-particle diffusion in the vertical direction behaves similarly to the one in the horizontal plane. It also displays two régimes and obeys

$$< \zeta_v^2(\tau) >= u'^2\tau^2 \tag{38}$$

in the τ^2-régime and

$$< \zeta_v^2(\tau) >= 2 < \zeta_h^2(\tau) >= 4\,Ro\,L^2\frac{\tau}{t_d} \tag{39}$$

in the $\tau-$régime (see figure 9).

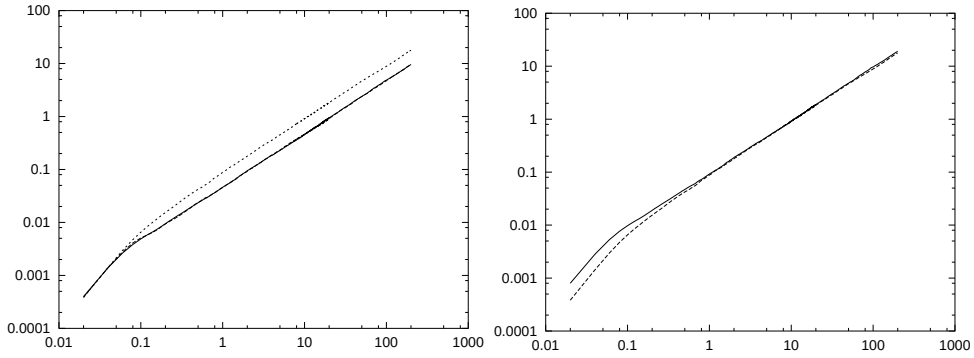

Fig. 8. One-particle mean square displacement as a function of τ/t_d in purely rotating turbulence for case A in table 2. Left: non-dimensional displacement $<\zeta_i^2>/L^2$, (i=1,2,3), as a function of τ/t_d; solid line and dashed line represent the horizontal diffusion ($i=1,2$), and dotted line is for the vertical diffusion ($i=3$). Right: solid line: twice the horizontal displacement $2<\zeta_h^2>/L^2$, dashed line: the vertical displacement $<\zeta_v^2>/L^2$.

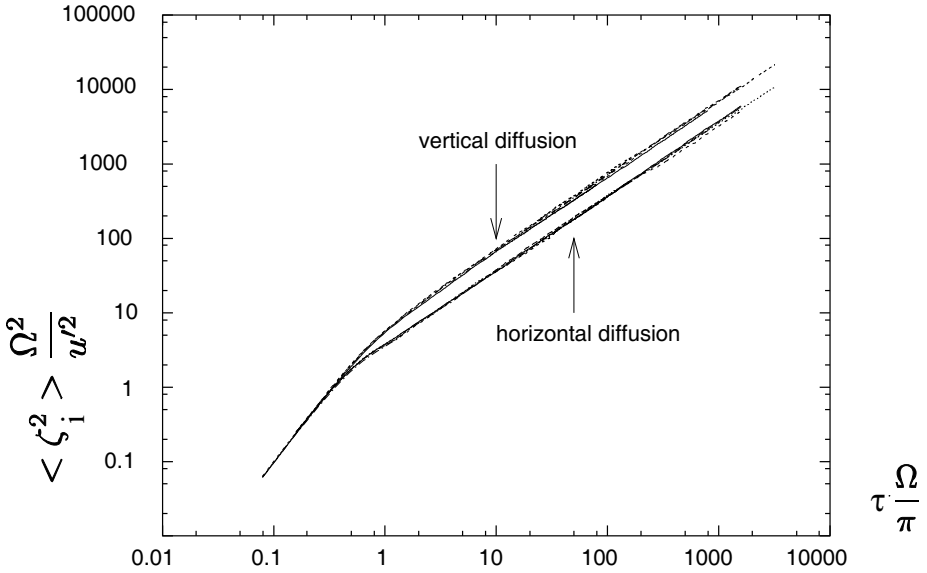

Fig. 9. Non-dimensional one-particle mean square horizontal $<\zeta_h^2>\Omega^2/u'^2$ and vertical $<\zeta_v^2>\Omega^2/u'^2$ displacements as functions of $\tau\Omega/\pi$ in purely rotating turbulence for cases A, B, C, D and E in table 2.

5 Two-particle diffusion in purely rotating turbulence

5.1 Two-particle diffusion in the τ^2- and $\tau-$régimes

Figure 10 shows that the two-particle diffusions in the two horizontal directions are statistically identical, $\delta_h^r(\tau)$ thus represents the two-particle mean square relative separation in any of the two horizontal directions. Both the vertical and the horizontal relative diffusions exhibit a τ^2-régime at small times and

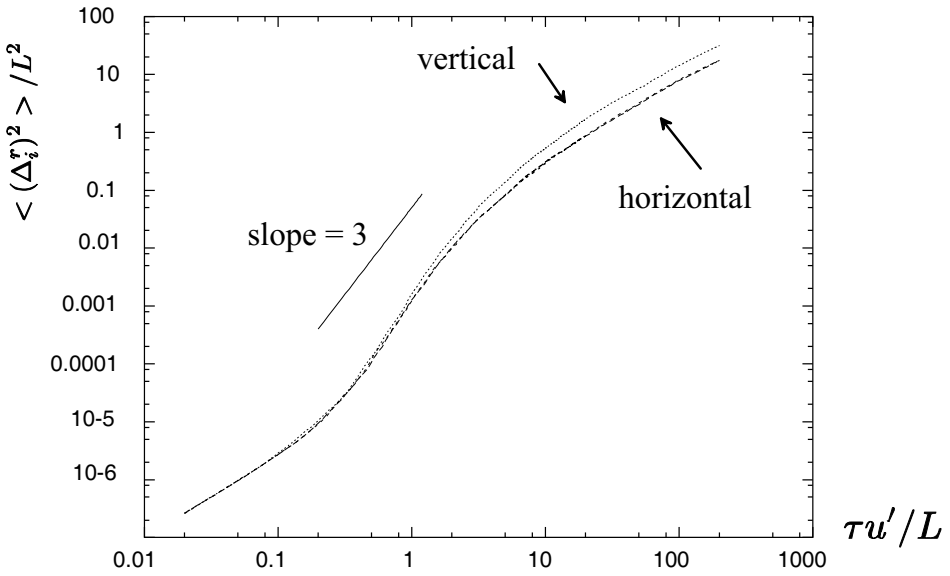

Fig. 10. Non-dimensional two-particle mean square relative separation $< \Delta_i^r(\tau)^2 > /L^2$, (i=1,2,3), as a function of $\tau u'/L$ in purely rotating turbulence for case F in table 2.

a $\tau-$régime at large times. In the τ^2-régime the diffusion is isotropic, as $\delta_h^r(\tau) = \delta_v^r(\tau)$. This isotropy is then broken at the end of the τ^2-régime when the horizontal relative diffusion becomes smaller than the vertical one. In the final $\tau-$régime, the asymptotic vertical diffusion becomes twice that of the horizontal one, $\delta_v(\tau)^2 = 2\delta_h(\tau)^2$.

The isotropic τ^2-régime can be explained in terms of a Taylor expansion when τ is small, which leads to

$$< \Delta_i^r(\tau)^2 > \simeq (\delta v_i)^2 \tau^2 \tag{40}$$

for $\tau \to 0$, where $\delta v_i = \sqrt{< \left(v_i^{(2)}(0) - v_i^{(1)}(0)\right)^2 >}$ is the initial characteristic velocity difference over the particle-pair. As noted by Cambon & Jacquin (1989) the initial isotropy of the velocity field is conserved by RDT and as a consequence it is also conserved by KS. Accordingly, for two single particles initially separated by $\Delta_i(0)$ their initial rms velocity difference δv_i is also isotropic and subscript i can be dropped in equation (40).

When the time is large enough, the particles of the pair eventually become independent and behave as two uncorrelated particles so that

$$< \Delta_i^r(\tau)^2 > = 2 < \zeta_i(\tau)^2 >$$

and using the results of §4.2, we retrieve the one-particle $\tau-$régime with a ratio of 2 between vertical and horizontal diffusion:

$$< \Delta_h^r(\tau)^2 > = \frac{1}{2} < \Delta_v^r(\tau)^2 > \tag{41}$$

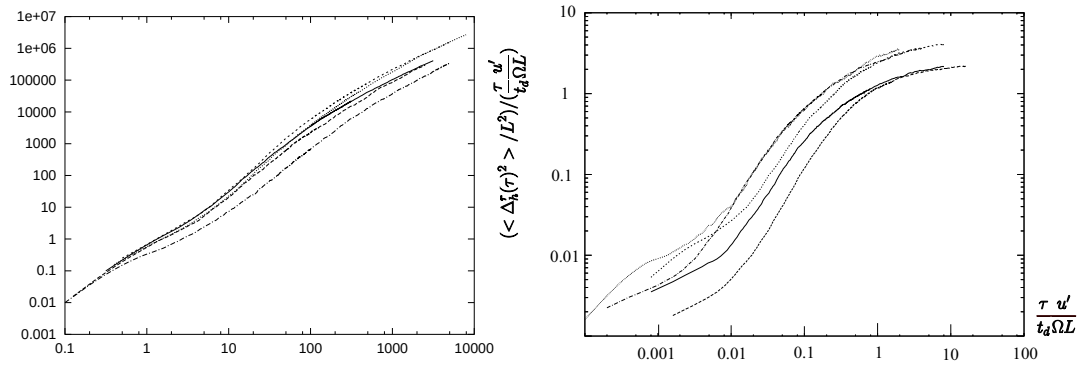

Fig. 11. Non-dimensional two-particle horizontal diffusion for cases A, B, C, D, E, and I in table 2. Left: $< \Delta_h^r(\tau)^2 > /(\delta v_h t_\eta)^2$ as a function of τ/t_η. Right: $< \Delta_h^r(\tau)^2 > /L^2/\frac{\tau}{t_d}\frac{u'}{\Omega L}$ as a function of $\frac{\tau}{t_d}\frac{u'}{\Omega L}$.

Thus, we validate that our KS predicts the two asymptotic τ^2- and $\tau-$régime. In figure 11, the different cases A, B, C, D, E, and I in table 2 are investigated. On the left, results are plotted in terms of the non-dimensional horizontal diffusion $< \Delta_h^r(\tau)^2 > /{\delta v_h}^2 t_\eta^2$ as a function of τ/t_η. The only effect of the angular velocity Ω in this régime is to be found in its duration which is a decreasing function of Ω.

We have tried different non-dimensional plots, a good collapse in the $\tau-$régime is also be observed for all the cases studied here when the results were plotted in terms of the non-dimensional horizontal diffusion $< \Delta_h^r(\tau)^2 > /L^2$ as a function of $\frac{\tau}{t_d}\frac{u'}{\Omega L}$ (not shown here).

On figure 11-right, in order to study the beginning of the $\tau-$régime we choose to plot $< \Delta_h^r(\tau)^2 > /L^2/\frac{\tau}{t_d}\frac{u'}{\Omega L}$ as a function of $\frac{\tau}{t_d}\frac{u'}{\Omega L}$. The figure shows the τ-regime as an asymptotic regime. A constant value of $< \Delta_h^r(\tau)^2 > /L^2/\frac{\tau}{t_d}\frac{u'}{\Omega L}$ is reached except in cases when we stopped the computation too early. Nevertheless, we can still say that the trend of these curves is the same: they are parallel from $\frac{\tau}{t_d}\frac{u'}{\Omega L} = 1$ on. So, it is just a matter of computation time for all the cases to reach the τ-regime and whatever the criteria we set for that they will arrive at a constant $< \Delta_h^r(\tau)^2 > /L^2/\frac{\tau}{t_d}\frac{u'}{\Omega L}$ at a same value of $\frac{\tau}{t_d}\frac{u'}{\Omega L}$.

We can conclude that the two-particle mean square horizontal diffusion in the $\tau-$régime is a function of the large scale turbulence parameters L, Ro and t_d, and that the time τ_{rw} when the $\tau-$régime appears is a function of both characteristic times $1/\Omega$ and L/u'. i.e.

$$\tau_{rw} \approx \left(\frac{L}{u'}\right)^2 \Omega \approx \frac{L}{u'}\frac{1}{Ro} \tag{42}$$

It is worth noting that equation (42) is not at odds with equation (35), for the nature of the τ-regime for one particle is very different from that for two. The beginning of the τ-regime for one particle is not due to the particle being

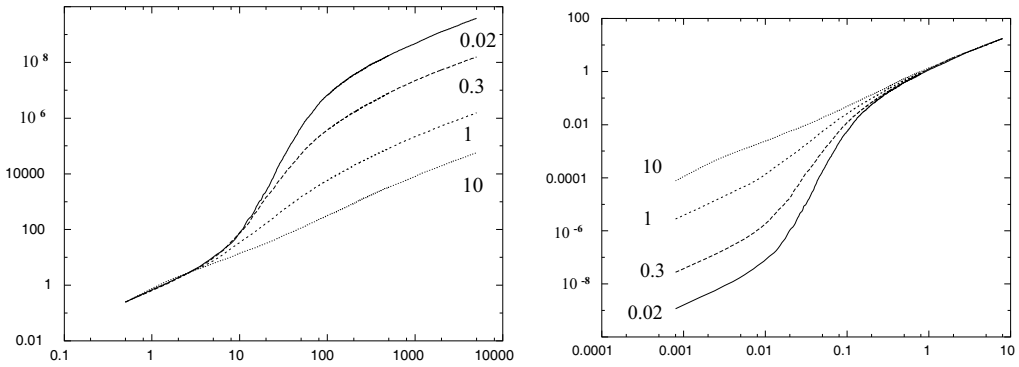

Fig. 12. Effect of Δ_0 on two-particle horizontal diffusion. Left: $< \Delta_h^r(\tau)^2 > /(\delta v_h t_\eta)^2$ as a function of $\frac{\tau}{t_\eta}$. Right: $< \Delta_h^r(\tau)^2 > /L^2$ as a function of $\frac{\tau}{t_d}\frac{u'}{\Omega L}$. Cases are G, F, A, and H in table 2 corresponding to Δ_0/η=0.02, 0.3, 1 and 10 as labelled.

decorrelated from its initial condition but is a pure effect of rotation, whereas the two particles reach a τ-regime when they become independent which is controlled by both turbulence and rotation characteristic times. (This is easier to analyse when rotation is superimposed on stratification (Nicolleau *et al.* (2006)).

So far the investigation has been restricted to varying turbulence parameters. Will the initial separation Δ_0 affect the scalings of these two régimes? In figure 12 left, the non-dimensional two-particle horizontal diffusion $< \Delta_h^r(\tau)^2 > /(\delta v_h t_\eta)^2$ is plotted as a function of τ/t_η for different initial separations $\Delta_0/\eta = 0.02$, 0.3, 1 and 10. In the same figure on the right, the two-particle horizontal diffusion results are presented in terms of $< \Delta_h^r(\tau)^2 > /L^2$ as a function of $\frac{\tau}{t_d}\frac{u'}{\Omega L}$; the long time scaling does not depend on the initial separation.

Figures 13 and 14 present similar results regarding the scalings of the two-particle vertical diffusion in the two régimes. We find that

$$\frac{< \Delta_i^r(\tau)^2 >}{L^2} = C_i \, Ro \, \frac{\tau}{t_d} \tag{43}$$

where $i = 1$, 2 and 3.

$$C_i = \begin{cases} 4 & \text{when } i = 1, 2 \\ 8 & \text{when } i = 3 \end{cases}$$

Again, these scalings are independent of the initial separation Δ_0.

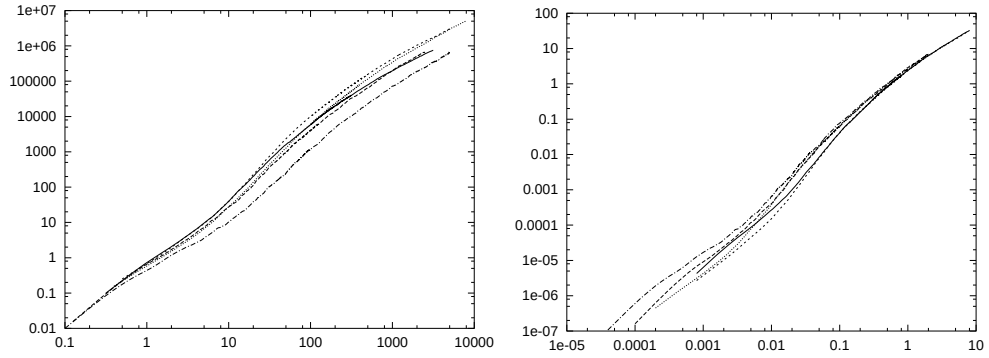

Fig. 13. Non-dimensional two-particle vertical diffusion for cases A, B, C, D, E, and I in table 2. Left: $< \Delta_v^r(\tau)^2 > /(\delta v_v t_\eta)^2$ as a function of τ/t_η. Right: $< \Delta_v^r(\tau)^2 > /L^2$ as a function of $\frac{\tau}{t_d}\frac{u'}{\Omega L}$.

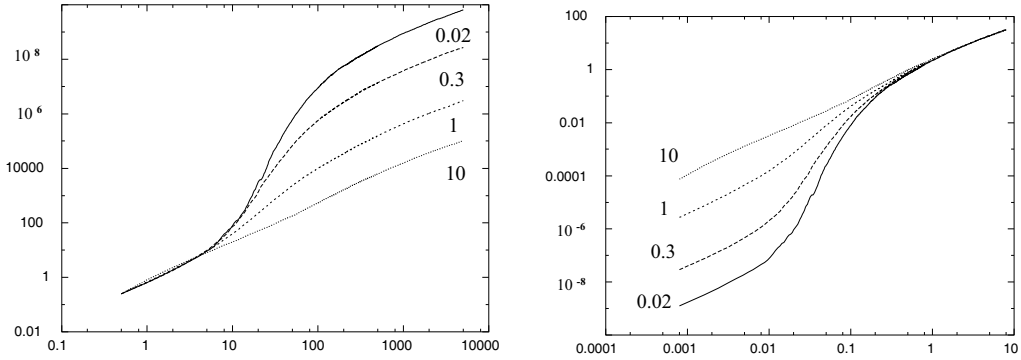

Fig. 14. Effect of Δ_0 on two-particle vertical diffusion. Left: $< \Delta_v^r(\tau)^2 > /(\delta v_v t_\eta)^2$ is plotted as a function of $\frac{\tau}{t_\eta}$. Right: $< \Delta_v^r(\tau)^2 > /L^2$ is plotted as a function of $\frac{\tau}{t_d}\frac{u'}{\Omega L}$. Cases from bottom to top are G, F, A, and H in table 2 corresponding to Δ_0/η=0.02, 0.3, 1 and 10 as labelled.

5.2 Two-particle diffusion at intermediate times and the locality-in-scale hypothesis for pure rotation

From all the figures presented in section 5.1, one can readily observe that the diffusion at intermediate times, i.e. the régime between the $\tau-$ and τ^2-régimes, is governed by a different law and is Δ_0-dependent. Next, it is worth asking

- whether the locality-in-scale hypothesis is still valid in purely rotating turbulence.
- Is the angular velocity Ω going to play a role in purely rotating turbulence as N does in purely stratified turbulence?
- Do the vertical and horizontal diffusions obey the same law in this régime?
- What are the effects of the initial separation?

A procedure similar to what has been undertaken for purely stratified tur-

bulence is to be employed here. The horizontal and vertical diffusions are investigated in terms of the two-particle diffusivity $\frac{d}{dt} < \Delta_i^2 >$ as functions of δ_i.

5.2.1 Pair horizontal diffusion and the locality-in-scale hypothesis for pure rotation

To study the effects of the rotation, cases J, O, P and Q in table 2 are examined. Case J is actually an isotropic case for the purpose of comparison. All the cases have a fixed $L/\eta = 125$ and share a same $\Delta_0/\eta = 0.1$ but have different Rossby numbers due to different Ω. Results are presented in figure 15 in terms of Richardson's coefficient β_h as a function of the r.m.s. separation δ_h/η. Compared with the isotropic case, the introduction of rotation generates a decrease in β_h, and its value is much closer to a constant indicating that the locality-in-scale hypothesis is better verified in the presence of rotation. It can also be seen that β_h is an increasing function of the Rossby number. Recalling that

$$\frac{d}{dt} < \Delta_h^2 >= \beta_h u' \eta \left(\frac{L}{\eta}\right)^{-1/3} \left(\frac{\delta_h}{\eta}\right)^{4/3}$$

one can say that a stronger rotation results in a weaker diffusion in the horizontal plane.

Figure 15 also shows that unlike pure stratified turbulence where stratification increases χ_h (the range over which the locality-in-scale hypothesis applies) up to scales outside the inertial subrange, rotation has no significant effect on χ_h.

When the Rossby number is constant, figure 16 displays another feature of the locality-in-scale hypothesis. The inertial subrange ratio L/η equals 500 for case K, 250 for case L and 125 for cases M and N. In this figure, all the curves collapse onto the line representing Richardson's four-third diffusivity law. Furthermore, a larger L/η corresponds to a longer collapse onto the line, and cases M and N are nearly identical throughout. One can therefore conclude that for a fixed Rossby number, χ_h in purely rotating turbulence behaves in a similar way to that in isotropic turbulence, i. e. χ_h is an increasing function of L/η.

5.2.2 Effect of the initial separation on the pair horizontal diffusion for purely rotating turbulence

So far, the discussion on two-particle horizontal diffusion for intermediate times has been based on a fixed value of the initial separation. Given a certain Rossby number, the dependence of β_h on Δ_0/η is shown in figure 17 where the corresponding isotropic cases are also plotted for the purpose of comparison. It shows that, when compared to the isotropic cases where Richardson's dif-

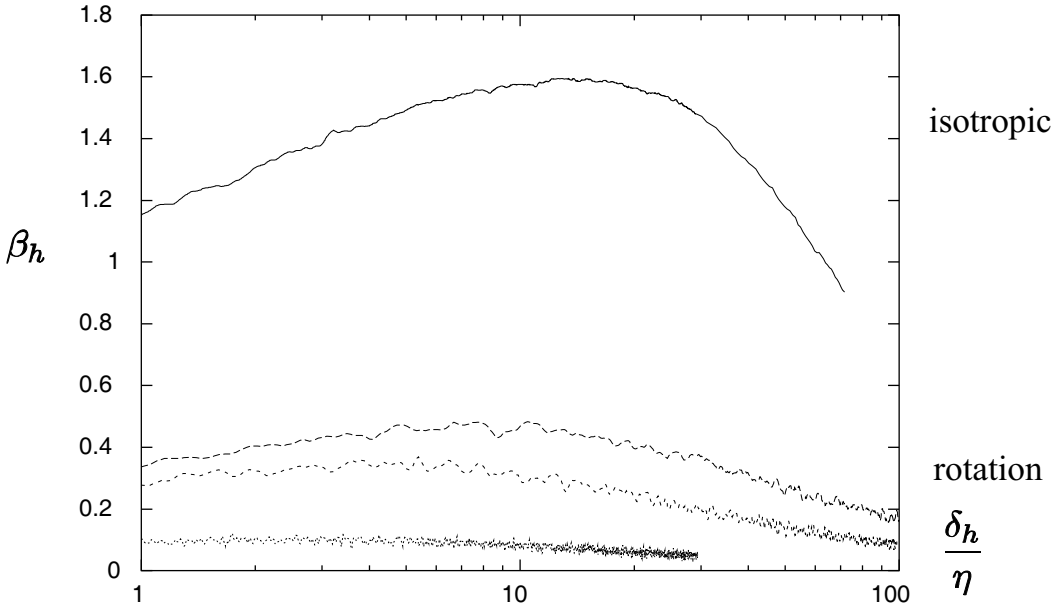

Fig. 15. β_h as a function of δ_h/η in purely rotating turbulence at a constant $\Delta_0/\eta = 0.1$. Curves from top to bottom are J, O, P and Q in table 2 corresponding to $Ro = \infty$, 0.04, 0.02 and 0.005 respectively.

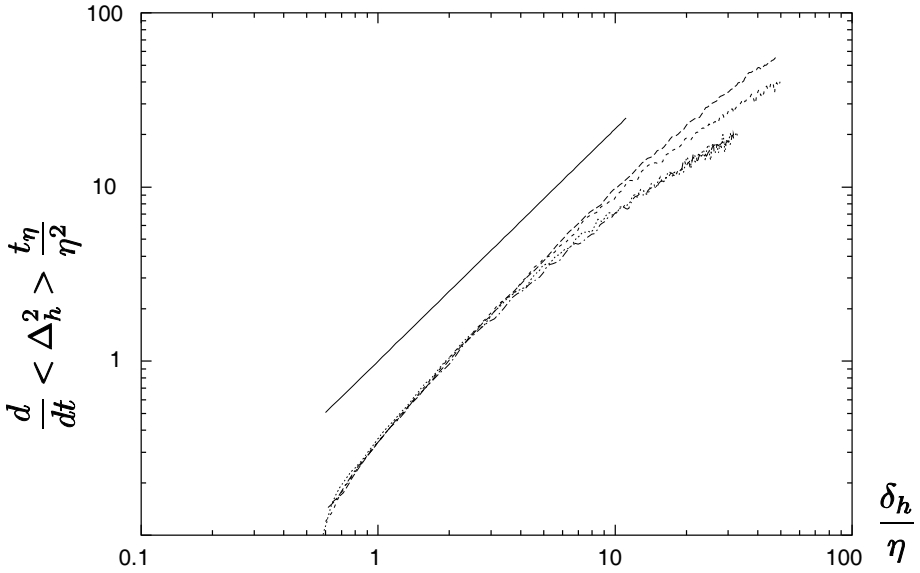

Fig. 16. Effects of L/η on two-particle horizontal diffusion. Non-dimensional horizontal diffusivity $\frac{d}{dt} < \Delta_h^2 > \frac{t_\eta}{\eta^2}$ is plotted as a function of δ_h/η in purely rotating turbulence for cases from top second to bottom K, L, M and N in table 2. Solid line represents Richardson's four-thirds diffusivity law in the horizontal plane.

fusivity law needs modifying for $\Delta_0/\eta \leq 1$, in purely rotating turbulence the variation of β_h with $\frac{\delta_h}{\eta}$ over the four-third diffusivity range can be ignored for initial separation much smaller than L. β_h is therefore δ_h-independent and as a consequence Richardson's diffusivity law is valid for any initial separation smaller than L. It can also be concluded that β_h is a weakly increasing func-

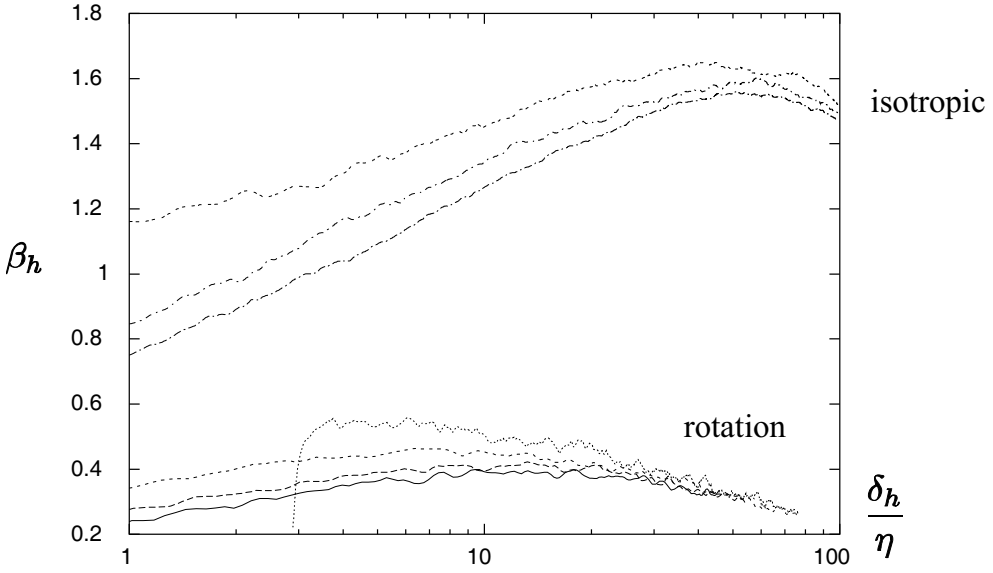

Fig. 17. β_h as a function of δ_h/η in purely rotating turbulence. Curves in the bottom group correspond to $\Delta_0/\eta = 0.02$, 0.1, 1 and 5 from bottom to top. (i. e. cases R, S, K and T in table 2). The corresponding isotropic cases are plotted in the top group where from bottom to top $\Delta_0/\eta = 0.02$, 0.1 and 1.

tion of Δ_0/η and that when $\Delta_0/\eta > 1$, χ_h is a function of Δ_0/η and decreases with it.

5.2.3 Pair vertical diffusion and locality assumption for purely rotating turbulence

Figure 18 demonstrates the relationship between the horizontal and the vertical diffusions. The diffusivities in the two directions are fairly closely matched in the inertial subrange. The only difference between them is that the vertical diffusion has a longer four-third diffusivity range. Richardson's diffusivity law (31) also applies to the vertical diffusion in purely rotating turbulence.

6 Conclusion

In this paper we use KS coupled with Rapid Distortion Theory to model one and two-particle diffusion in turbulence with stratification or rotation.

One-particle and two-particle diffusion is investigated for purely rotating turbulence. When $\tau \to 0$, one-particle horizontal and vertical diffusions follow the same τ^2-régime:

$$< \xi_i^2 >= u'^2 \tau^2$$

At large time $\tau \gg t_d$, the vertical diffusion is twice the horizontal one and

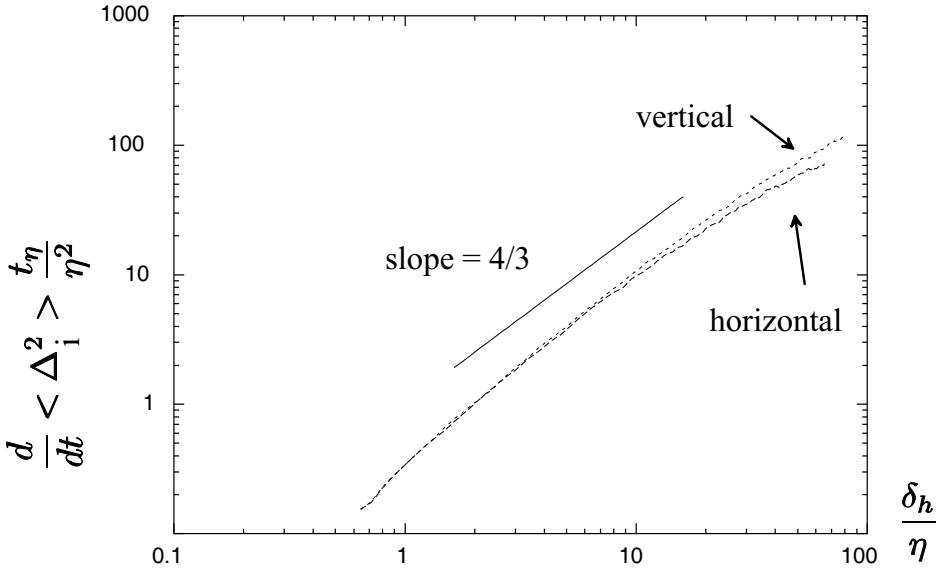

Fig. 18. Comparison of two-particle horizontal and vertical diffusions in purely rotating turbulence. $\frac{d}{dt} < \Delta_i^2 > \frac{t_\eta}{\eta^2}$ is plotted as a function of δ_i/η (i=h, v). Case L in table 2 is studied. The solid line with a slope of 4/3 represents Richardson's four-third diffusivity law.

both diffusions follow a τ-régime:

$$\frac{< \xi_v^2 >}{L^2} = 2\frac{< \xi_h^2 >}{L^2} = Ro\frac{\tau}{t_d}$$

Two similar régimes are found for pair diffusion in purely rotating turbulence: when $\tau \to 0$ the pair's horizontal and vertical diffusions follow the same τ^2-régime

$$< \Delta_i^r(\tau)^2 >= \delta v_i^2\, \tau^2$$

Whereas at large times, $\tau > Ro\, t_d$, the vertical diffusion is twice the horizontal one and both follow a τ-régime.

In the intermediary range of times, emphasis is made on the investigation of the locality-in-scale hypothesis in purely stratified and purely rotating turbulence. We adopt Nicolleau & Yu (2004)'s approach and study

$$\beta = \frac{\frac{d<\Delta^2>}{dt}}{u' \left(\frac{L}{\eta}\right)^{-\frac{1}{3}} \left(\frac{\delta}{\eta}\right)^{\frac{4}{3}}}$$

as a function of $\frac{\delta}{\eta}$. The dependence of β on $\frac{\delta}{\eta}$ is a measure of the departure from the locality assumption. We conclude that:

- For both rotation and stratification the coefficient β is an increasing function of the pair initial separation.
- In the case of pure stratification β is independent of N and χ the range of

scales over which the locality assumption is valid is extended outside the inertial range of scales.

- In the case of pure rotation β is an increasing function of the Rossby number, it has the same value for vertical and horizontal diffusions and the rotation does not alter much χ.

Acknowledgments

FN and GY acknowledge EPSRC sponsorship N° GR/N22601, GR/S95633/01, EPSRC UK Turbulence Consortium and GR/R64957/01, JCV acknowledges financial support from the Royal Society. We thank Claude Cambon for fruitful discussions during the writing of the paper.

References

Batchelor, G. K. 1952 The effect of homogeneous turbulence on material lines and surfaces. *Proc. Roy. Soc. London A* **213**, 349.

Bellet, F., Godeferd, F. S., Scott, J. F. & Cambon, C. 2006 *J. Fluid Mech.* **to appear**.

Cambon, C., Godeferd, F. S., Nicolleau, F. & Vassilicos, J. C. 2004 Turbulent Diffusion In Rapidly Rotating Turbulence With or Without Stable Stratification. *J. Fluid Mech.* **499**, 231–255.

Cambon, C. & Jacquin, L. 1989 Spectral approach to non-isotropic turbulence subjected to rotation. *J. Fluid Mech* **202**, 295.

Cot, C. 2001 Equatorial mesoscale wind and temperature fluctuations in the lower atmosphere. *J. Geophys. Res.* **106** (D2), 1523–1532.

Elliott, F. W. & Majda, A. J. 1996 Pair dispersion over an intertial range spanning many decades. *Phys. Fluids* **8** (4), 1052–1060.

Flohr, P. & Vassilicos, J. C. 2000 Scalar subgrid model with flow structure for large-eddy simulations of scalar variances. *J. Fluid Mech.* **407**, 315–349.

Fung, J. C. H., Hunt, J. C. R., Malik, N. A. & Perkins, R. J. 1992 Kinematic Simulation of homogeneous turbulence by unsteady random Fourier modes. *J. Fluid Mech.* **236**, 281–317.

Fung, J. C. H. & Vassilicos, J. C. 1998 Two-particle dispersion in turbulentlike flows. *Phys. Rev. E* **57** (2), 1677–1690.

Godeferd, F. & Staquet, C. 2003 Statistical modelling and direct numerical simulations of decaying stably-stratified turbulence. *J Fluid Mech.* **486**, 115–150.

Godeferd, F. S. & Cambon, C. 1994 Detailed investigation of energy transfers in homogeneous stratified turbulence. *Phys. Fluids* **6**, 2084–2100.

Godeferd, F. S., Malik, N. A., Cambon, C. & Nicolleau, F. 1997 Eulerian and Lagrangian Statistics in Homogeneous Stratified Flows. *Applied Scientific Research* **57**, 319–335.

Kaneda, Y. & Ishida, T. 2000 Suppression of vertical diffusion in strongly stratified turbulence. *J. Fluid Mech.* **402**, 311–327.

Kimura, Y. & Herring, J. R. 1996 Diffusion in stably stratified turbulence. *J. Fluid Mech.* **328**, 253–269.

Kimura, Y. & Herring, J. R. 1999 Particle dispersion in rotating stratified turbulence. *Proceedings of FEDSM99* **FEDSM99-7753**.

Liechtenstein, L., Cambon, C. & Godeferd, F. 2006 Nonlinear formation of structures in rotating stratified turbulence. *Journal of Turbulence* **6** (24), 1–18.

Lindborg, E. 2002 Srongly stratified turbulence: A special type of montion. In *Advanced in Turbulence IX, Proceedings of the Ninth European Turbulence Conference* (ed. I. P. Castro, P. E. Hancock & T. G. Thomas), pp. 435 – 442. CIMNE.

Malik, N. A. & Vassilicos, J. C. 1996 Eulerian and Lagrangian Scaling Properties of Randomly Advected Vortex tubes. *J. Fluid Mech.* **326**, 417–436.

Morel, P. & Larchevêque, M. 1974 Relative Dispersion of Constant-Level Balloons in the 20mb General Circulation. *J. Atm. Sc.* **31**, 2189.

Nastrom, G. D. & Gage, K. S. 1985 A Climatology of Atmospheric Wavenumber Spectra of Wind and Temperature Observed by Commerical Aircraft. *J. Atmos. Sci.* **42**, 950–960.

Nicolleau, F. & ElMaihy, A. 2004 Study of the development of a 3-D material surface and an iso-concentration field using KS. *J. Fluid Mech.* **517**, 229–249.

Nicolleau, F. & Vassilicos, J. C. 2000 Turbulent diffusion in stably stratified non-decaying turbulence. *J. Fluid Mech.* **410**, 123–146.

Nicolleau, F. & Vassilicos, J. C. 2003 Turbulent Pair Diffusion. *Phys. Rev. Letters* **90** (2), 024503.

Nicolleau, F. & Yu, G. 2004 Two-particle diffusion and locality assumption. *Phys. Fluids* **16** (4), 2309–2321.

Nicolleau, F., Yu, G. & Vassilicos, J. C. 2006 Turbulence with combined stratification and rotation, limitations of Corrsin's hypothesis. *Phys Rev. E* p. to be submitted.

Obukhov, A. M. 1941 On the distribution of energy in the spectrum of turbulent flow. *Bull. Acad. Sci. U.S.S.R, Géog. & Géophys., Moscow* **5**, 453–466.

Osborne, D. R., Vassilicos, J. C., Sung, K. & Haigh, J. D. 2006 Fundamentals of pair diusion in kinematic simulations of turbulence. *Physical Review E* **in press**.

Praud, O., Fincham, A. M. & Sommeria, J. 2005 Decaying grid turbulence in a strongly stratified fluid. *Journal of Fluid Mech.* **522**, 1–33.

Thomson, D. J. & Devenish, B. J. 2005 Particle pair separation in kine-

matic simulations. *J. Fluid Mech.* **526**, 277–302.

Yokokawa, M., Itakura, K., Uno, A., Ishihara, T. & Kaneda, Y. 2002 16.4-Tflops Direct Numerical Simulation of Turbulence by a Fourier Spectral Method on the Earth Simulator. In *Conference on High Performance Networking and Computing*, pp. 1–17. Proceedings of the 2002 ACM/IEEE conference on Supercomputing, Baltimore, Maryland USA.